ACS OMEGA

Open Access

http://pubs.acs.org/journal/acsodf

Article

Catalytic Thermocuring and Synergistic Photothermocuring of Single-Component Acrylate-Grafted Liquid Oligosilazanes

Keke Pei, Sen Li, Biwen Cao, Mingcun Wang,* and Mingjie Liu

Cite This: *ACS Omega* 2024, 9, 24959−24969

Read Online

ACCESS | Metrics & More | Article Recommendations

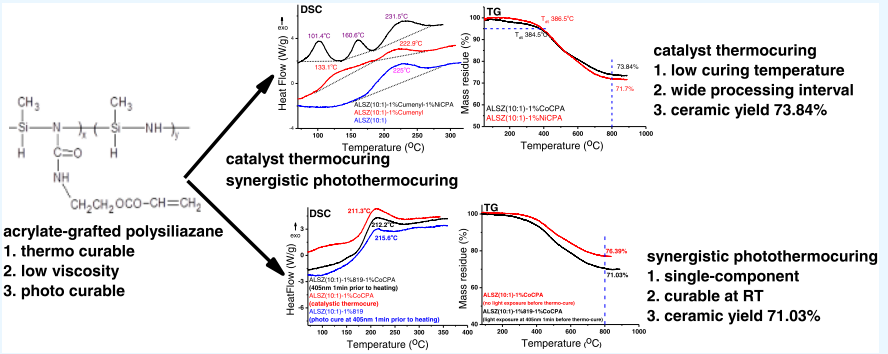

ABSTRACT: A novel thermosetting preceramic resin called acrylate-grafted liquid polysilazane (ALSZ) was readily synthesized. The curing behaviors of ALSZ were investigated by the techniques of differential scanning calorimetry (DSC), thermogravimetric analysis (TGA), and rheological tests. The catalytic thermocuring process was controlled by the addition of a polymerization accelerator composed of a radical initiator (cumene hydroperoxide) and a transition metal catalyst (nickel naphthenate or cobalt naphthenate). Photocuring at room temperature can proceed readily by the addition of photosensitizer 819 (phenylbis(2,4,6-trimethylbenzoyl) phosphine oxide). By combining a radical initiator, a transition metal catalyst, and a photosensitizer, synergistic photothermocuring was achieved, demonstrating advantages such as material shaping at room temperature and low weight loss during curing. The ceramization of the solidified ceramic precursors in an Ar atmosphere was studied using TGA and tube furnace pyrolysis. ALSZs exhibited comparatively high ceramic transformation yields (71−75% at 800 °C). The resulting pyrolytic ceramics maintained their original shape without deformation or foaming expansion. Polysilazanes containing acrylate groups can directly form casting bodies, showing a high static glass transition temperature (>380 °C) by thermomechanical analysis (TMA). FT-IR analyses revealed that multiple reactions are involved in the curing of ALSZ. The results in this paper showed that ALSZ might find prospective applications in material processing, such as additive manufacturing and ceramic−matrix composites.

1. INTRODUCTION

Nonoxide ceramics and ceramic−matrix composites, such as silicon carbide, silicon nitride, and silicon carbonitride, etc., have been finding extensive applications in the fields of electronics, information technology, aerospace, and other high-tech industries,[1,2] because of their distinguished characteristics such as corrosion resistance,[3] high-temperature resistance,[4] high hardness, and low coefficient of thermal expansion.[5] Although ceramic−matrix composites exhibit excellent high-temperature strength and oxidation resistance,[6] the preparation process of such materials is intricate, time-consuming, and costly;[7] furthermore, nonoxide ceramics and their composites face intrinsic shortcomings, such as low toughness and micropores.[8] Currently, the prevalent method for preparing ceramic−matrix composites is based on organic polymer precursors that undergo recyclable precursor infiltration and pyrolysis (PIP) to transform the polymeric matrix into inorganic ceramics.[9,10]

Polysilazane, a commonly utilized nonoxide ceramic precursor, is frequently employed in the realm of coatings and ceramic fibers,[11] albeit with limitations pertaining to their size and thickness. Wang et al. prepared a fluorine-free, protective, hydrophobic, crosslinked ceramizable coating of polysilazane through deamination by air moisture.[12] Yang et al. successfully synthesized SiCuCN-based nanocomposites by the SSP method via nucleophilic substitution reactions at the Si

Received: February 29, 2024
Revised: April 24, 2024
Accepted: May 15, 2024
Published: June 2, 2024

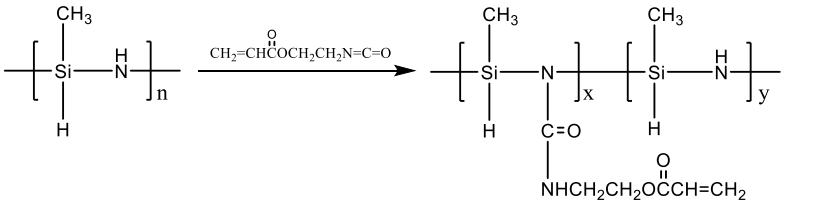

molar ratio

y:x	ALSZdesignation
2:1	ALSZ(2:1)
5:1	ALSZ(5:1)
10:1	ALSZ(10:1)
20:1	ALSZ(20:1)

Figure 1. Molecular structure of ALSZ with varying acrylate contents.

centers of PSZ.[13] Zhang et al. synthesized cobalt-containing polysilazane nanofibers with fluorescence by electrospinning.[14] However, materials with polysilazane as the resin matrix have been rarely reported due to the absence of proper curing methods to form well-shaped monoliths.[15] Generally, the transamination condensation of polysilazane occurs at temperatures as high as 300 °C,[16] and it is nearly impossible to achieve one solidified material with a prefixed shape and size. The reported crosslinking of polysilazane at room temperature is usually carried out by moisture hydrolysis, which results in the final polymer containing the silica−oxygen structure that is suitable only for coating and painting.[17] The curing of polysilazane can be primarily classified into two categories: thermal curing and UV curing. Thermal curing involves the crosslinking of polysilazane monomers to form a crosslinking network under scheduled heating conditions facilitated by a free radical initiator or a metallic catalyst. Conversely, UV curing entails the addition of a photosensitizer to induce the crosslinking of polysilazane even at room temperature and create a crosslinking network through exposure to UV light in a short time.

Our research aims at chemically modifying the present polysilazane with isocyanate acrylate ethyl acetate in order to enhance their thermal curability and light curability and improve their resistance performance at high temperatures. In this paper, a cost-effective catalytic thermocuring method is employed to convert liquid acrylate-grafted oligosilazane (ALSZ) efficiently into a solid with low mass loss by using the combination of a transition metal catalyst (nickel naphthenate or cobalt naphthenate) and a radical initiator (cumene hydroperoxide). Furthermore, to the best of our knowledge, a synergistic photothermocuring method is first studied in this paper, in which UV radiation initiates the radical polymerization of acryl side groups at room temperature to gelate ALSZ, and the complete three-dimensional network is entirely formed via the subsequent catalytic thermocuring reactions of hydrocoupling between Si−H and N−H. Such a synergistic curing method endows the cured monolithic ALSZ with a precise shape, with nearly no mass loss, so this mild and environmentally benign curing method is highly desirable for the construction of engineering and functional polysilazane-based materials.

Recently, additive manufacturing of preceramics for pyrolysis to ceramic metamaterials has been attracting the attention of several researchers, and therefore, photosensitive polysilazanes, including single-component and reactive blending, have been investigated.[18] Chen et al. presented a novel strategy for fabricating lightweight SiCN amorphous ceramics with electrical semiconducting behaviors through digital light processing (DLP).[19] Hoffmann et al. investigated the resource-efficient curing of polyorganosilazane-based coating via photocuring.[20] Dandan Ren et al. studied the influences of the bifunctional acrylic reactive diluent tripropylene glycol diacrylate content, photoinitiator concentration, and temperature on the UV-curing polymerization rate and conversion percentage of the liquid polyborosilazane.[21] Currently, the photocuring of polysilazanes is typically achieved through the blending of vinyl-containing polysilazanes and photocurable resins (such as acrylate), resulting in a multicomponent system.

For the above multicomponent photocurable vinyl polysilazane systems, because of the differences in the radical polymerization reactivity in the copolymerization of acryl and vinyl groups (e.g., reactivity ratio ≠1), the inconsistent and ever-changing polymerization rate for each group will lead to a variance of crosslinked structures in different parts and at different times.[22] However, single-component acrylate-grafted oligosilazane (ALSZ) will possibly dissipate the above problems. Therefore, in this paper, we will investigate the curing formula, curing behaviors, and curing mechanism of ALSZ, with the preceramic-to-ceramic conversion yield as another research focus. The research in this paper will provide a single-component thermosetting polysilazane with UV curability and catalytical curability that will meet the demands of processing methods such as light-curable additive manufacturing, prepreg laminates, etc.

2. EXPERIMENTAL SECTION

2.1. Materials and Reagents. Oligosilazane was self-made in our laboratory by the ammonolysis of methyldichlorosilane, trimethylchlorosilane, and methyltrichlorosilane. It was obtained as a light-yellow liquid at room temperature with a viscosity of ∼30 mPa·s. Cobalt naphthenate acid (CoCPA; Co 7.8−8.2%), nickel naphthenate acid (NiCPA; Ni 8%), cumene hydroperoxide solution (cumenyl; 85%), and photosensitizer 819 (phenylbis 2,4, 6-trimethylbenzoyl phosphine oxide; 98%) were all provided by Shanghai McLean Biochemical Technology Co. Ltd.

2.2. Synthesis of Acrylate-Grafted Oligosilazane (ALSZ) with Varying Acrylate Contents. By adding 2-isocyanatoethyl acrylate into oligosilazane dropwise under adequate stirring, the synthesis process is conducted at room temperature in a nitrogen atmosphere to ensure isolation from air and moisture. After reaction for 24 h, the viscous yellow liquid of ALSZ can be used for the next step. The scheme of the chemical reaction between oligosilazane and 2-isocyana-

https://doi.org/10.1021/acsomega.4c02018
ACS Omega 2024, 9, 24959−24969

toethylaacrylate is exhibited in Figure 1; acryl groups were grafted on polysilazane through the hydrogen-transfer addition reaction of isocyano and N−H.

By adjusting the content of acrylate, various ALSZ (with molar ratios of the silazane unit and acrylate unit as 20:1, 10:1, 5:1, and 2:1) were synthesized and labeled as ALSZ(20:1), ALSZ(10:1), ALSZ(5:1), and ALSZ(2:1), respectively, as shown in Figure 1.

2.3. Catalytic Thermocuring Samples of ALSZ. The free radical initiator cumene hydroperoxide (cumenyl) and catalyst nickel naphthenate acid (NiCPA) were added according to a prefixed proportion of the mass fraction of ALSZ, mixed evenly, and placed in an alumina crucible. The crucible containing the sample was placed into the furnace for thermal curing under argon gas protection according to the following protocol: 70 °C 0.5 h → 130 °C 0.5 h → 170 °C 0.5 h → 230 °C 1 h → cooling down freely. A dense, dark-brown solid was obtained. When the catalyst CoCPA was used, the curing process was carried out following the same method.

Preceramic samples with different formulations are named according to the format "ALSZ−cumenyl−catalyst". For example, if the sample is composed of ALSZ(10:1), 1% free radical initiator cumenyl, and 1% catalyst NiCPA, the sample is named "ALSZ(10:1)−1% cumenyl−1% NiCPA".

2.4. Synergistic Photothermocuring Samples of ALSZ. The radical initiator cumenyl, the catalyst NiCPA, and photosensitizer 819 (phenylbis 2,4,6-trimethylbenzoyl phosphine oxide) were added according to a prefixed proportion of the mass fraction of ALSZ, mixed evenly, and put into an alumina crucible. The sample in the crucible was cured by UV irradiation at 405 nm for 1 min at room temperature, and then the crucible containing the sample was placed into a furnace for thermal curing under argon gas protection according to the following protocol: 70 °C 0.5 h → 130 °C 0.5 h → 170 °C 0.5 h → 230 °C 1 h → cooling down freely. A dense dark-brown solid was obtained. When the catalyst CoCPA was used, the curing process was carried out following the same method.

The prepared preceramic samples were named according to the format "ALSZ−photosensitizer−cumenyl−catalyst". For example, the sample composed of ALSZ(10:1), 1 wt % photosensitizer 819, 1 wt % free radical initiator cumene hydroperoxide, and 1 wt % catalyst nickel naphthenate acid is named "ALSZ(10:1)−1%819−1% cumenyl−1% NiCPA".

2.5. Catalytic Thermocuring Samples of ALSZ(10:1) for FT-IR Analysis of the Curing Mechanism. The free radical initiator cumenyl and catalyst CoCPA were added according to a prefixed proportion of the mass fraction of ALSZ and mixed evenly. The samples were divided into seven parts, out of which six parts were cured in the tube furnace for 1 h under argon flow at temperatures of 70, 130, 170, 200, 230, and 300 °C, respectively.

2.6. Characterizations. Differential scanning calorimetry (DSC) and thermogravimetric analysis (TGA) were performed on a Netzsch STA449F3 thermal analyzer with argon gas at 50 mL/min and a heating rate of 10 °C/min. The ceramization of the cured preceramic resins was carried out in the high-temperature furnace AFD-2.5−12 under a flowing argon atmosphere, and the pyrolysis was scheduled as follows: RT → 800 °C (heating time 2 h) → 800 °C (holding time 1 h) → RT (cool down freely). Thermomechanical analysis (TMA) was performed on a heat engine analyzer TMA7100 under an air atmosphere at a heating rate of 5 °C/min. The rheological test was conducted using an MCR 702e under a strain of 1%, an angular frequency of 10 rad/s, and a heating rate of 5 °C/min. The FT-IR spectra were collected over a range of 500−4000 cm^{-1} on an iCAN9 (Tianjin Neng-pu, China) FT-IR spectrometer at RT, using KBr pellets, with a scanning time of 16 and a resolution of 4 cm^{-1}.

3. RESULTS AND DISCUSSION

3.1. Effects of the Acrylate Content on the Curing Temperature and Mass Loss on Thermal Curing. In order to trace the progress of the hydrogen-transfer addition reaction between LSZ and 2-isocyanatoethyl acrylate in ALSZ synthesis, FT-IR spectroscopy (absorbance−wavenumber spectrum) was employed to characterize ALSZ at different reaction times to detect the conversion rate of isocyanate groups. The absorbance of isocyanate groups was normalized based on the absorbance of the silicon hydrogen bond as an internal standard, and the results of the isocyanate conversion rate versus reaction time are shown in the embedded table in Figure 2. The synthesis is almost completed at 24 h at room temperature, with only 11.8% isocyanate groups left. Upon increasing the reaction time, the conversion rate of isocyanates slowly increases to level off. The remaining isocyanates can be further reduced by heating at 70 °C for 1 h if a rapid synthesis is required. ALSZ is a transparent yellow liquid with a viscosity of approximately 100−300 mPa·s at RT, depending on the acrylate content. As such, the successful synthesis of single-component photocurable acrylate-grafted polysilazanes was confirmed.

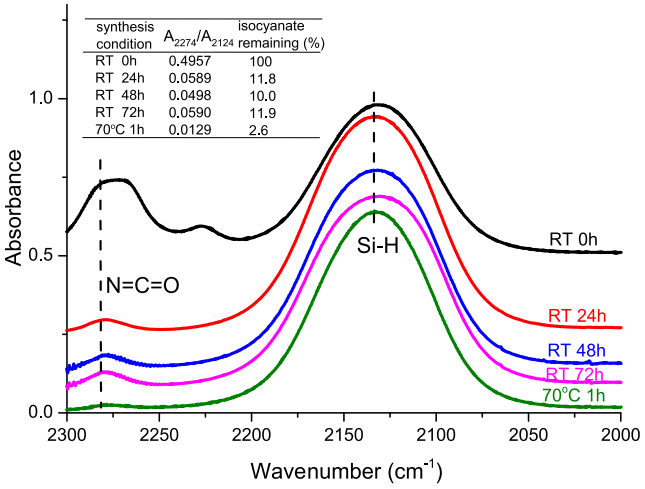

Figure 2. FT-IR (absorbance−wavenumber) spectra of ALSZ(10:1) at different reaction times between oligosilazane and 2-isocyanatoethyl acrylate.

The acrylate content in ALSZ significantly affects thermal curing behaviors, which can be demonstrated by the methods of DSC and TGA. Figure 3 shows the DSC and TGA curves of the catalytic thermocuring process of ALSZ with different acrylate contents, and Table 1 shows the temperature peak and weight loss in catalytic thermocuring. In Figure 3, with an increase in the acrylate content, the main curing peak temperature increased and the enthalpy (indicated by the corresponding peak area) increased remarkably. With an increase in the acrylate content in ALSZ, under the curing accelerator composed of cumene hydroperoxide and nickel naphthenate acid, below 200 °C, the exothermic peaks shifted

https://doi.org/10.1021/acsomega.4c02018
ACS Omega 2024, 9, 24959−24969

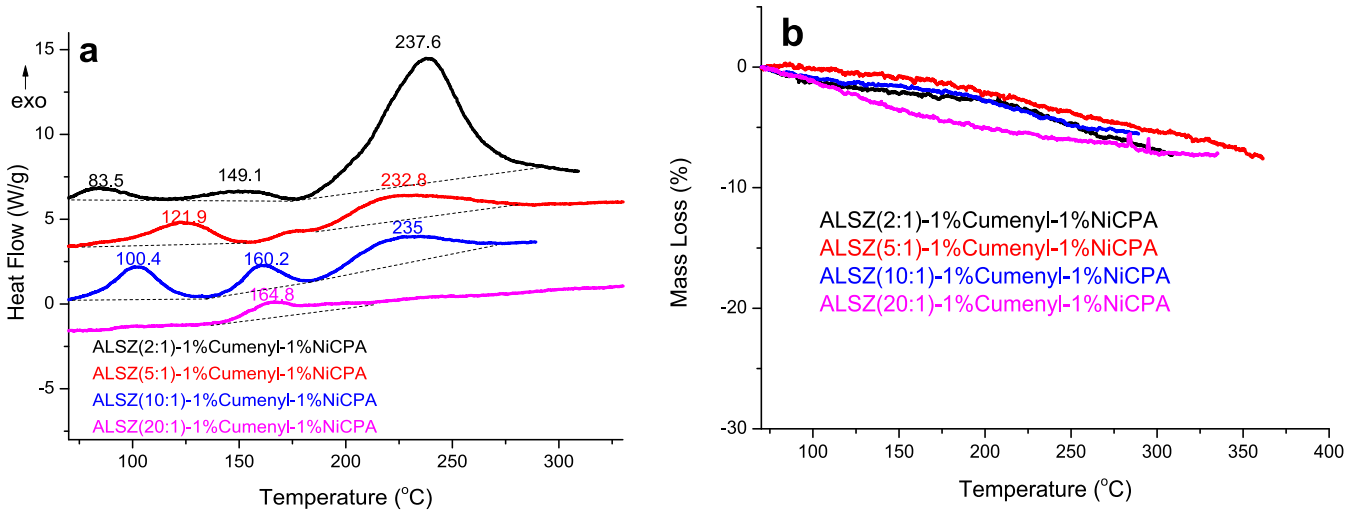

Figure 3. DSC and TGA profiles of ALSZ−cumenyl−NiCPA containing different amounts of acrylate groups. (a) DSC profiles of the catalytic thermocuring process. (b) TGA profiles of mass loss during curing.

Table 1. Curing Peaks and Curing Mass Loss of ALSZ−Cumenyl−NiCPA Containing Different Amounts of Acrylate Groups

preceramic resin formulation	curing peaks by DSC	curing mass loss by TGA until 300 °C
ALSZ(2:1)−1%cumenyl−1%NiCPA	83.5 °C, 149.1 °C, 237.6 °C	−7.66%
ALSZ(5:1)−1%cumenyl−1%NiCPA	121.9 °C, 232.8 °C	−5.12%
ALSZ(10:1)−1%cumenyl−1%NiCPA	100.4 °C, 160.2 °C, 235 °C	−5.43%
ALSZ(20:1)−1%cumenyl−1%NiCPA	164.8 °C	−4.70%

to a lower temperature because of the existence of more reactive acrylate groups initiated by redox radical polymerization, which can proceed at highly reduced temperatures. However, above 200 °C, the position of the main exothermic peak exhibited a higher enthalpy due to normal radical polymerization.[23]

Ascertained by TG curves and the mass loss data in Table 1, with an increase in the acrylate content in ALSZ, the weight loss during the catalytic thermocuring of ALSZ also increased from −4.70 to −7.66%. This implies that the introduction of acrylate leads to a little more volatility during the catalytic thermocuring process.

The successful synthesis of single-component acrylate-grafted polysilazanes offers a cost-effective route for the preparation of UV-curable preceramics in the polymer-to-ceramic technique. The reduced curing temperature and minimal weight loss during the curing process of acrylate-grafted polysilazanes hold promising implications for the fabrication of large-sized materials.

3.2. Effect of the Free Radical Initiator and Catalyst on the Curing Behaviors of ALSZ. It is crucially important to understand the effect of the free radical initiator (cumene hydroperoxide) and the catalyst (cobalt naphthenate acid or nickel naphthenate acid) on the curing behaviors of ALSZ so

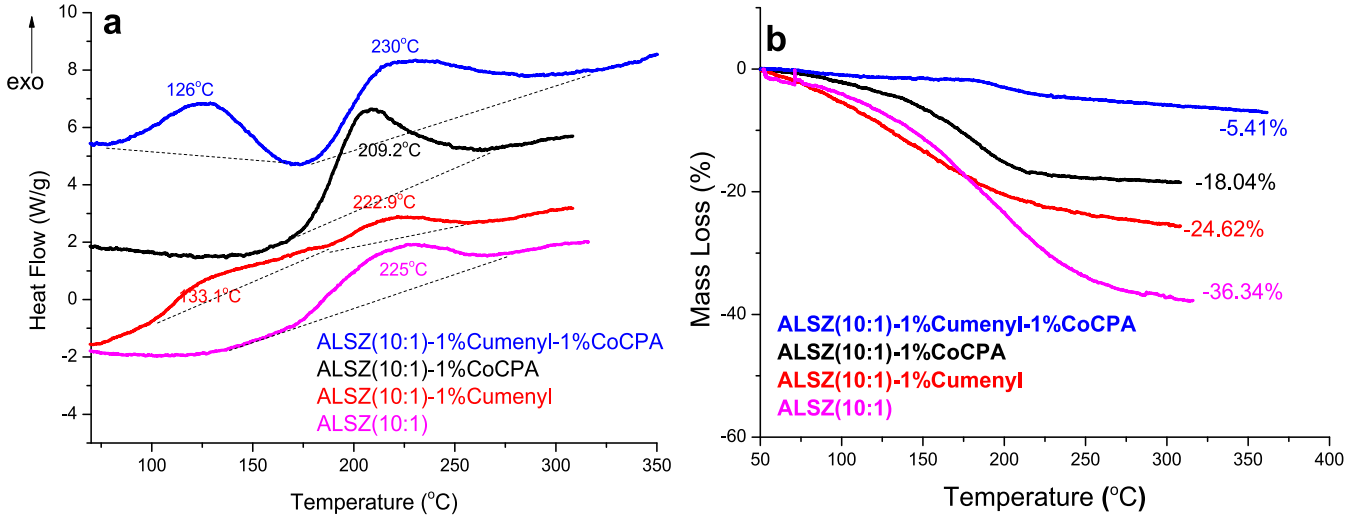

Figure 4. DSC and TGA profiles of ALSZ(10:1) with different curing reagents while CoCPA was used. (a) DSC profiles of curing processes. (b) TGA profiles of mass loss during the curing processes.

https://doi.org/10.1021/acsomega.4c02018
ACS Omega 2024, 9, 24959−24969

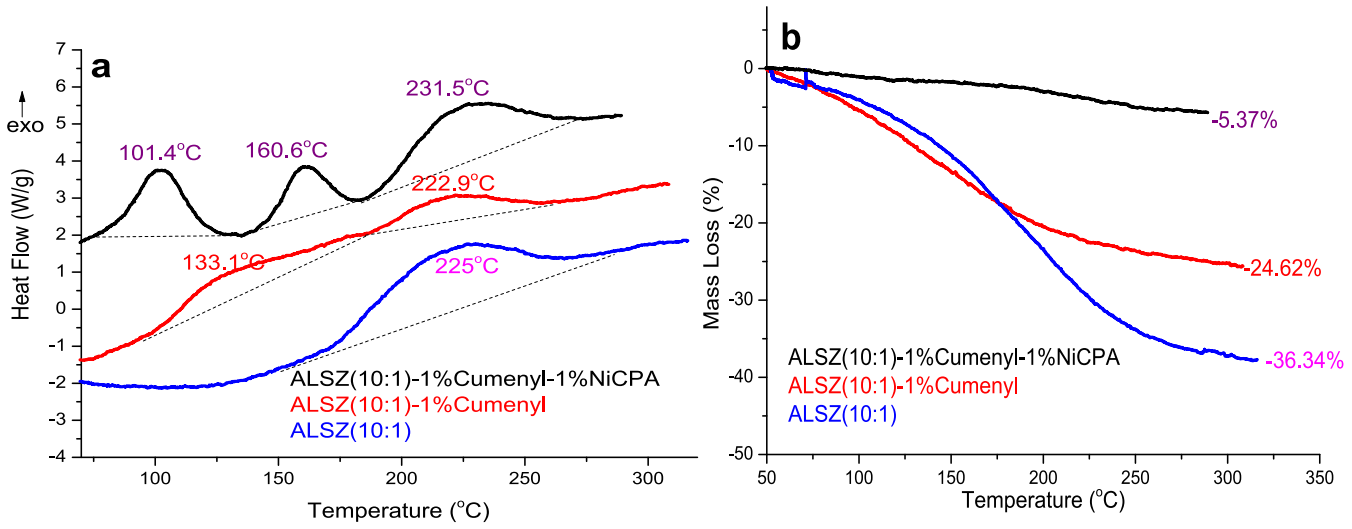

Figure 5. DSC and TGA profiles of ALSZ(10:1) with different curing reagents while NiCPA was used. (a) DSC profiles of the curing processes. (b) TGA profiles of mass loss during the curing processes.

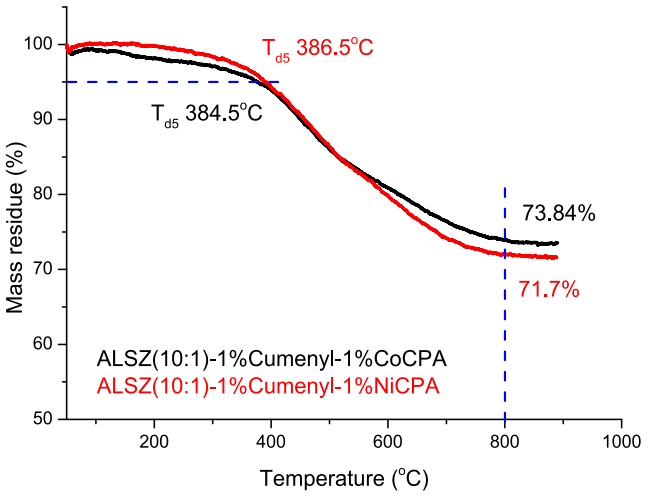

Figure 6. TGA profiles of cured ALSZ(10:1)−cumenyl−CoCPA and ALSZ(10:1)−cumenyl−NiCPA.

as to process the preceramic resin readily at mild conditions into size-precise and complex-shaped materials.

Figure 4 shows the DSC curves and TGA curves of the catalytic thermocuring process of ALSZ with different formulations when the transition metal catalyst is cobalt naphthenate acid (CoCPA). In the DSC diagrams, the following results can be shown clearly: (1) When only CoCPA was added in plain ALSZ, the exothermic peak was reduced from 225 to 209.2 °C, together with a remarkably increased enthalpy, indicating the strong catalysis of CoCPA for crosslinking reactions of ALSZ. (2) When cumene hydroperoxide was added as the radical initiator, almost no change was recorded in the peak temperature of radical polymerization compared with that of plain ALSZ (10:1), and the enthalpy was nearly comparable. (3) When cobalt naphthenate acid and cumene hydroperoxide were added simultaneously, the catalytic thermocuring process involved two highly exothermic reactions, one peaking at 126 °C and the other at 230 °C; the lower peak is caused by redox radical polymerization and dehydrogenation,[24] while the higher peak is caused by normal radical polymerization.

The TG diagrams reveal the following results of mass loss during different curing processes: (1) CoCPA resulted in a decrease in weight loss of ALSZ during the curing process from 36.34 to 24.62%, while cumene hydroperoxide exhibited a further reduction to 18.04%. When CoCPA or cumene hydroperoxide was used, owing to the highly reduced curing temperature, the three-dimensional crosslinking network grows rapidly, avoiding the volatilization loss of the uncured small molecules. (2) When CoCPA and cumenyl were added simultaneously, the weight loss upon catalytic thermocuring was drastically reduced to 5.41%. This could be attributed to the curing reaction at <126 °C, which suppressed further weight loss during the subsequent heating.

In previous research, nickel acetylacetonate was applied as an effective catalyst to thermally cure polysilanes[25] and polysilazanes,[26] respectively. However, the powder of Ni(acac)2 was hardly resolved in polysilazane. As such, in this paper, liquid organonickel or organic cobalt compounds were chosen as catalysts, showing complete miscibility with ALSZ and a highly efficient polymerization catalytic effect. Figure 5 shows the DSC and mass loss curves of catalytic thermocuring of ALSZ(10:1) when NiCPA was used. The figure demonstrates that NiCPA exhibits polymerization behaviors comparable to that of CoCPA, but the exothermic peaks exhibited a more complex profile (101.4, 160.6, and 231.5 °C).

Table 2. Curing Peaks, Curing Mass Loss, and Ceramic Yields of ALSZ(10:1)−Cumenyl−CoCPA

preceramic resin formulation	curing peaks by DSC	curing mass loss by TGA	ceramic yields at 800 °C in Ar by TGA
ALSZ(10:1)−1%cumenyl−1%CoCPA	129 °C, 230.2 °C	−6.56%	75%
ALSZ(10:1)−1%cumenyl−0.5%CoCPA	125.4 °C, 225 °C	−8.51%	73.8%
ALSZ(10:1)−1%cumenyl−0.25%CoCPA	150.5 °C, 233.3 °C	−6.53%	74.7%
ALSZ(10:1)−1%cumenyl−0.1%CoCPA	161.1 °C, 234.1 °C	−6.37%	71.3%

https://doi.org/10.1021/acsomega.4c02018
ACS Omega 2024, 9, 24959−24969

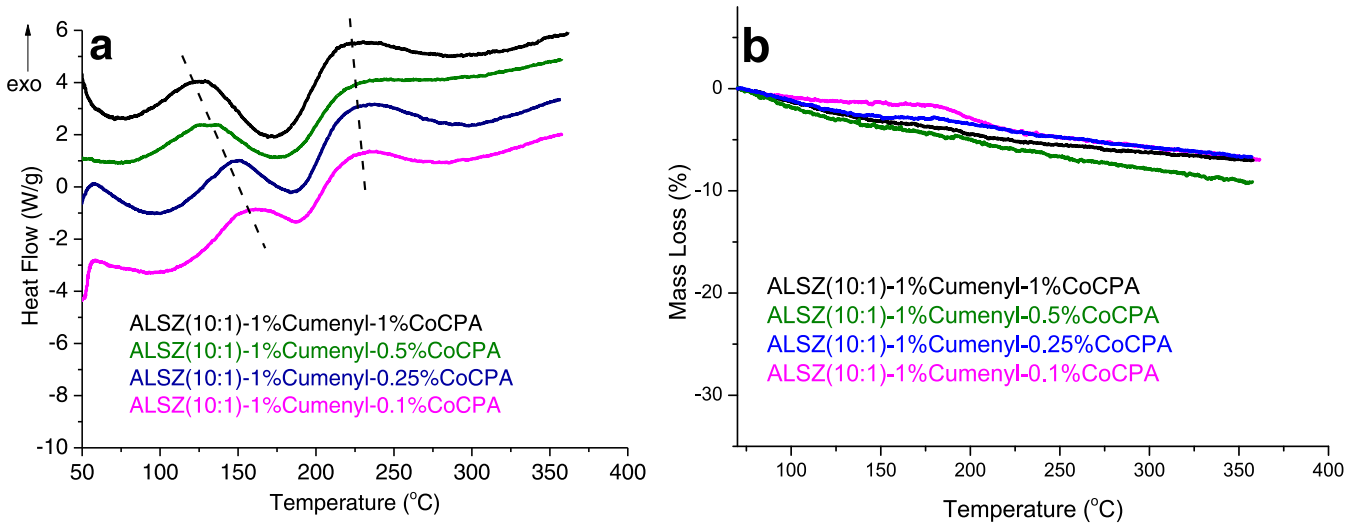

Figure 7. DSC and TGA profiles of ALSZ(10:1)−cumenyl−CoCPA. (a) DSC profiles of catalytic thermocuring. (b) TGA profiles of mass loss during catalytic thermocuring.

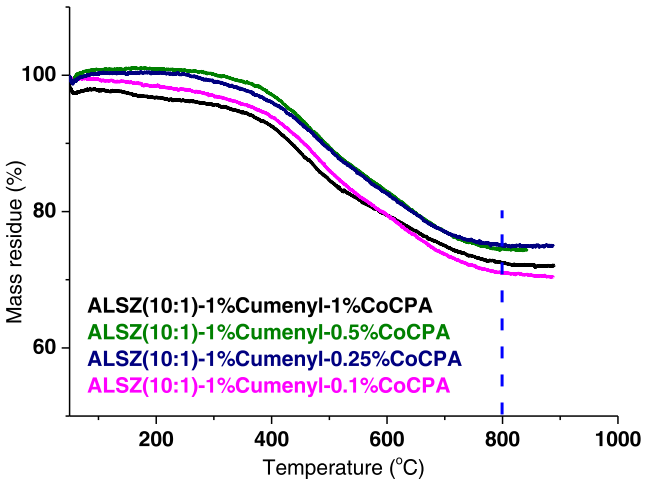

Figure 8. TGA profiles of the cured ALSZ(10:1)−cumenyl−CoCPA.

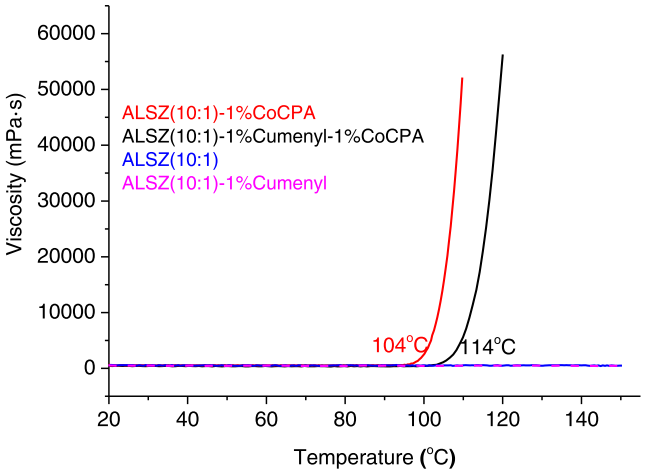

Figure 9. Rheological curves of ALSZ(10:1)−cumenyl−CoCPA.

Furthermore, there is negligible disparity in terms of the thermal curing weight loss. The above results show the similar catalytic capabilities of NiCPA and CoCPA, but it should be

Figure 10. Images of the cured ALSZ(10:1)−1%cumenyl−0.5% CoCPA casting body (top image) and its pyrolytic ceramic monolith after pyrolysis at 800 °C (bottom image).

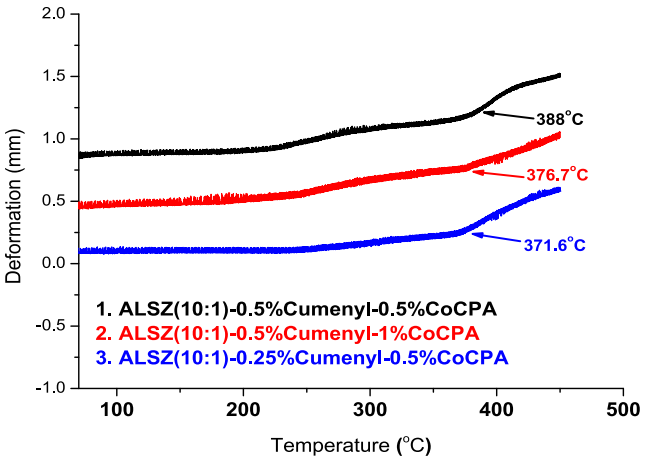

Figure 11. Thermomechanical analysis of cured ALSZ(10:1)−cumenyl−CoCPA.

pointed out that the pale color of cured ALSZ catalyzed by CoCPA is more attractive in most application circumstances.

To further compare the ceramic transformation yields after catalytic thermocuring of ALSZ(10:1) catalyzed by CoCPA and NiCPA, respectively, the TGA curves of the cured ALSZ(10:1)−1%cumenyl−1%CoCPA and ALSZ(10:1)−1% cumenyl−1%NiCPA are shown in Figure 6. The values of

https://doi.org/10.1021/acsomega.4c02018
ACS Omega 2024, 9, 24959−24969

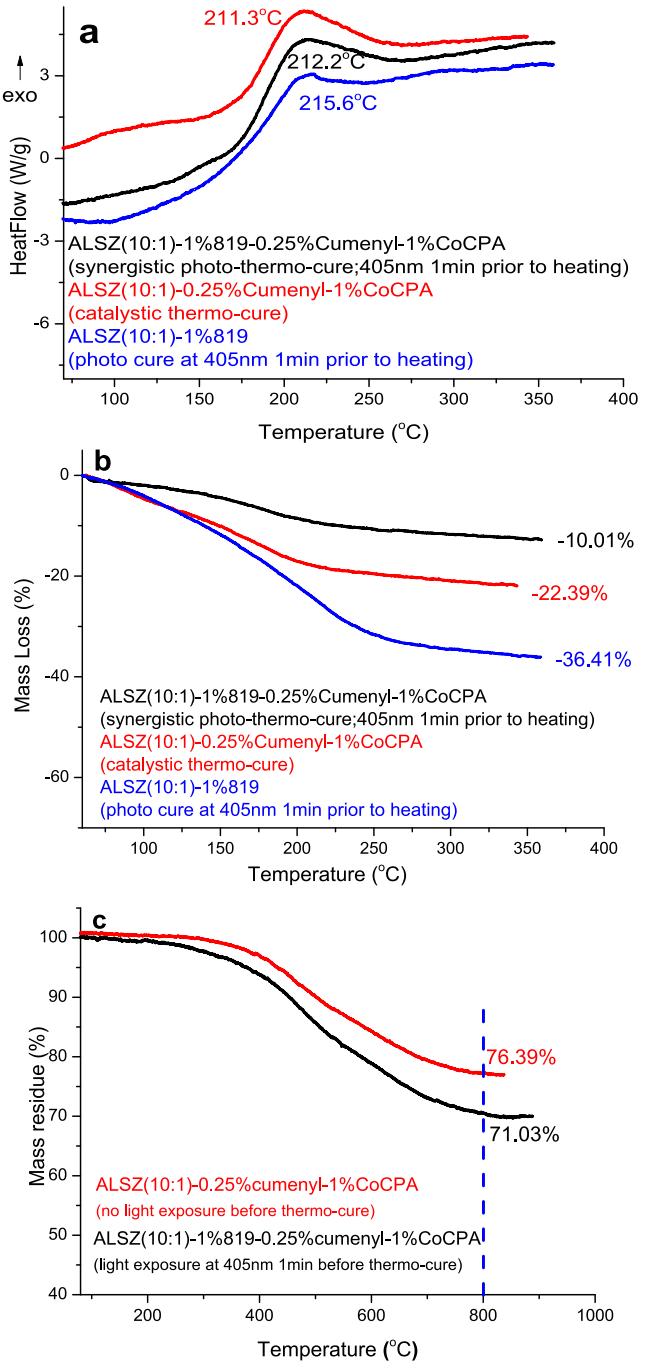

Figure 12. Photosensitizer effect on the curing behavior and ceramization yield of ALSZ(10:1). (a) DSC profiles of synergistic photothermocuring for ALSZ(10:1). (b) Mass loss in the synergistic photothermocuring of ALSZ(10:1). (c) TGA profiles of the cured samples of ALSZ(10:1)−819−cumenyl−CoCPA and ALSZ(10:1)−cumenyl−CoCPA.

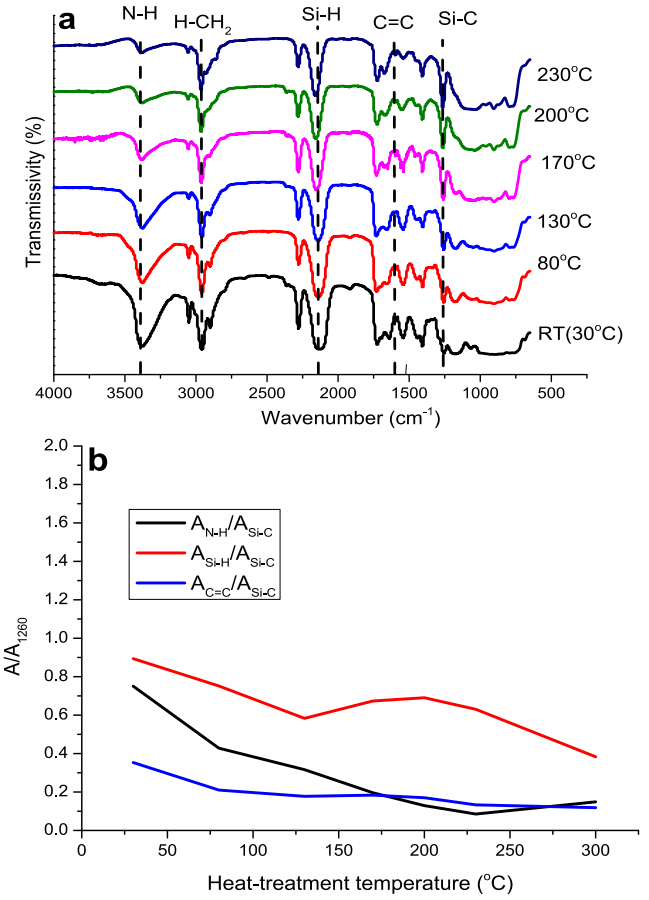

Figure 13. FT-IR analysis for the catalytic thermocuring of ALSZ(10:1)−1%cumenyl−0.5%CoCPA. (a) FT-IR spectra at various temperatures. (b) Profiles of the absorbance ratio versus heat treatment temperature for N−H, Si−H, and C═C bonds, respectively.

temperature with a mass loss of 5% (T_{d5}) of ALSZ(10:1)−1% cumenyl−1%CoCPA and ALSZ(10:1)−1%cumenyl−1% NiCPA were found to be 384.5 and 386.5 °C, respectively. The ceramic conversion yields of ALSZ(10:1)−1%cumenyl− 1%CoCPA and ALSZ(10:1)−1%cumenyl−1%NiCPA were 73.84 and 71.7%, respectively, which indicates that there is a high and similar ceramic conversion rate after catalytic thermocuring. CoCPA resulted in a slightly higher ceramic conversion rate (73.84%) than NiCPA, indicating that CoCPA exhibits slightly more effective catalysis for ALSZ ceramization. The ceramic yield was also verified by the tube furnace sintering experiment (at 800 °C under an argon atmosphere, the pyrolyzed ceramic yield of ALSZ(10:1)−1%cumenyl−1% CoCPA was found to be 75.6%, while the pyrolyzed ceramic yield of ALSZ(10:1)−1%cumenyl−1%NiCPA was found to be 75%), which was consistent with the results obtained by TGA.

When the amount of radical initiator cumene hydroperoxide was fixed at 1 wt %, Figure 6 shows the DSC and mass loss curves of the catalytic thermocuring of ALSZ with varying amounts of the CoCPA catalyst. In Table 2, the data on curing peak temperatures and curing weight loss are provided. The data presented in Figure 7 demonstrate a consistent decrease in the initial curing temperature (in the range of 100−190 °C) with an increase in the CoCPA catalyst amount, while the second curing temperature is observed at a similar position (in the range of 190−275 °C). The first peak and its trend are attributed to the redox radical polymerization of acrylate and the catalytic dehydrogenation of Si−H and N−H; the higher the amount of catalyst in ALSZ, the higher the reactivity of the cumenyl−CoCPA redox initiator and dehydrogenation;[24] therefore, the first peak shifted to a lower temperature. In contrast, with increasing concentration of CoCPA, the second peak occurred at a similar temperature with slight fluctuation due to the normal radical polymerization initiated by cumene hydroperoxide itself. The weight loss during catalytic

https://doi.org/10.1021/acsomega.4c02018
ACS Omega 2024, 9, 24959−24969

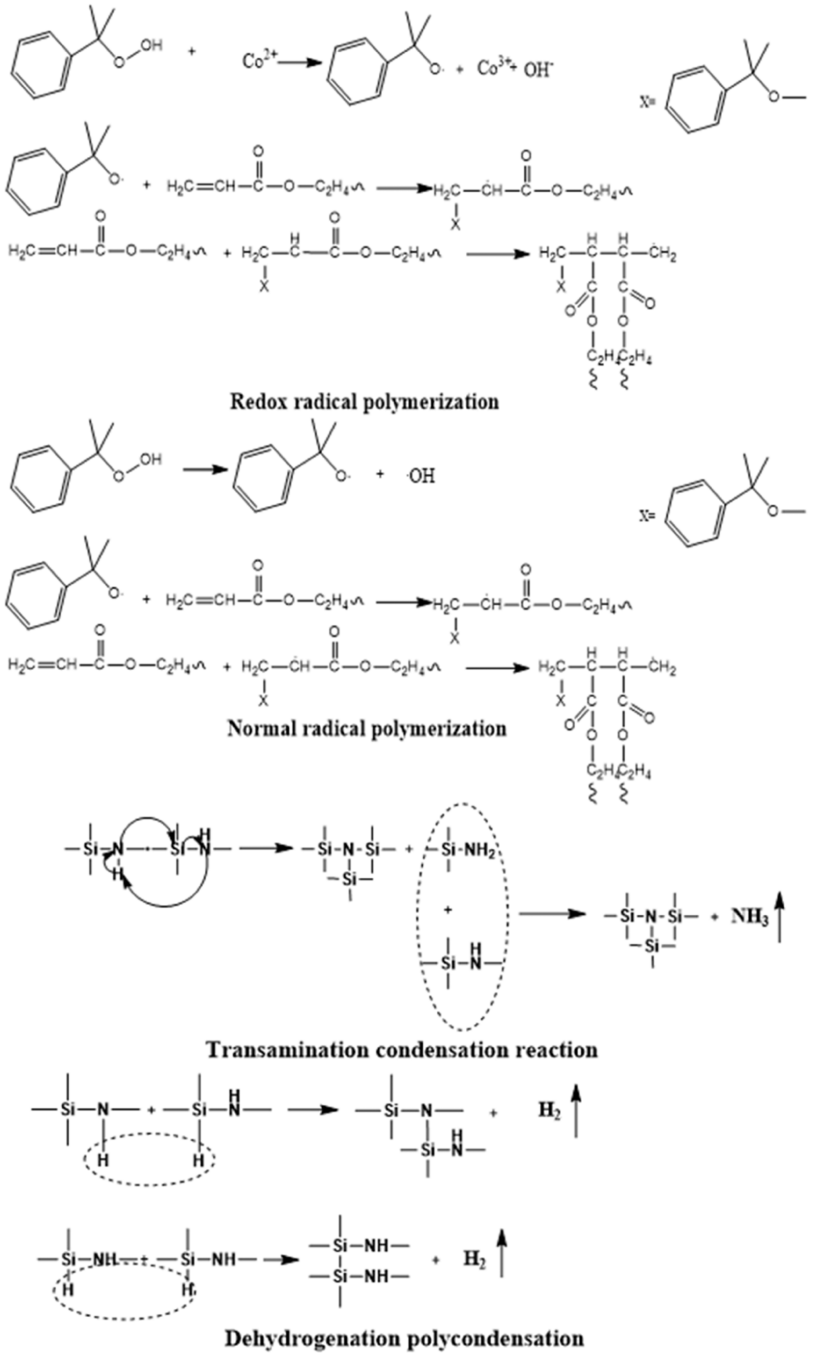

Figure 14. Probable mechanisms of catalytic thermocuring of ALSZ(10:1).

thermocuring was observed to be significantly low (<9%), with minimal influence of the concentration of the CoCPA catalyst.

Figure 8 shows TGA curves of the catalytically thermocured ALSZ(10:1)−cumenyl−CoCPA under an argon atmosphere, and the data of ceramization yields are also presented in Table 2. It can be found that with an increase in the CoCPA concentration in ALSZ, the cured ALSZ(10:1) showed a trend of a slight increase in the ceramic conversion yield. The ceramic yield was also verified by a tube furnace sintering test (at 800 °C, under an argon atmosphere, the pyrolyzed ceramic yield of ALSZ(10:1)−1%cumenyl−1%CoCPA was found to be 72%, that of ALSZ(10:1)−1%cumenyl−0.5%CoCPA was found to be 73.2%, and that of ALSZ(10:1)−1%cumenyl−0.25%CoCPA was found to be 71.4%). Therefore, a small amount of CoCPA catalyst in the ALSZ formulation is highly efficient in improving the thermal curing properties and ceramic conversion yield.

To investigate the correlation between viscosity and temperature in the presence of the radical initiator cumene hydroperoxide and catalyst CoCPA, dynamic rheological analyses were performed, as shown in Figure 9. It can be observed that both ALSZ(10:1) and ALSZ(10:1)−cumenyl exhibited negligible changes in viscosity throughout the entire measurement range until 150 °C, indicating slow network growth and an absence of gel formation. However, upon addition of the CoCPA catalyst, a significant increase in viscosity was observed for ALSZ(10:1)−1%CoCPA at 104 °C and for ALSZ(10:1)−1%cumenyl−1%CoCPA at 114 °C.

https://doi.org/10.1021/acsomega.4c02018
ACS Omega 2024, 9, 24959−24969

These phenomena indicate the high efficiency of the catalyst for the formation of crosslinked gels within the system, leading to a steep increase in viscosity. It is crucial to formulate processing parameters to control thermal curing in material manufacturing.

As a ceramic precursor thermosetting resin, the low curing temperature and high ceramic conversion yield of ALSZ serve as core indicators in applications of ceramic precursors. Because of its adjustable processing conditions, ALSZ also meets all kinds of processing methods in the fabrication of ceramics and their composites.

3.3. Thermomechanical Properties of the Casting Body of ALSZ. Thermomechanical properties are always decisive factors for new materials to pave pathways to civil and military engineering applications. In this paper, ALSZ(10:1)−1%cumenyl−0.5%CoCPA was used to prepare casting bodies through catalytic thermocuring using cumene hydroperoxide as an initiator and CoCPA as the catalyst. The casting body depicted in Figure 10 exhibits a well-defined size and shape; after pyrolysis at 800 °C under an inert atmosphere, the derived ceramic retained a well-defined monolithic form with about 21% size shrinkage, devoid of any porosity or cracks in visual appearance.

TMA curves of the cured samples are shown in Figure 11, and the inflection point on the curve of the deformation temperature is the static glass transition temperature (T_g). The T_g of the casting bodies exceeds 370 °C, with the highest recorded value reaching 388 °C. A comparison of ALSZ(10:1)−0.5%cumenyl−0.5%CoCPA and ALSZ(10:1)−0.5%cumenyl−1%CoCPA shows that the higher the amount of catalyst used, the lower the T_g presented. A comparison of ALSZ(10:1)−0.25%cumenyl−0.5%CoCPA and ALSZ(10:1)−0.5%cumenyl−0.5%CoCPA shows that the higher the amount of radical initiator used, the higher the T_g presented. Therefore, the optimized formulation of ALSZ succeeds in achieving a high glass transition temperature.

Meanwhile, the variation in the thickness of the test samples was very small (<10%) even at the test-end temperature until 450 °C. The high-temperature deformation resistance and small size shrinkage make ALSZ an ideal candidate in high-temperature material preparation, for example, polymer-based ceramizable materials utilized in a wide temperature range from RT (polymer materials) to high temperatures (in-situ-ceramized materials), which has been attracting ever-increasing interest in some high-tech engineering fields such as electronics and aerospace.[15]

3.4. Effect of Photosensitizer 819 on the Curing Behaviors of ALSZ. Photosensitive preceramic resins can be photocured under ambient conditions conveniently, which makes them widely used for coatings and stereolithography.[27] Here, we conduct a primary study on the synergistic photothermocuring of ALSZ in order to develop it for possible applications in additive manufacture (SLA or DLP).

Photosensitizer 819 was incorporated into the ALSZ(10:1) system and photopolymerization was initiated at room temperature; upon exposure to a violet lamp at 405 nm, a gel-like solid with sufficient strength was formed in seconds. Subsequently, a post heat treatment was conducted at elevated temperatures to completely crosslink the photocured gel into a hard solid.

As depicted in Figures 12a and 10b, for ALSZ(10:1), it can be observed that light exposure has less influence on the subsequent exothermic behaviors, but it is really an instructive result that the weight loss during the thermal curing process was significantly reduced from −22.4 to −10% with prior light exposure. This suggests that the small molecules within the system became immobilized in a three-dimensional network, resulting in decreased weight loss.

Then, to investigate the influence of the photosensitizer on the curing process of the plain ALSZ without cumene hydroperoxide and CoCPA therein, ALSZ was directly blended with photosensitizer 819 for the determination of its DSC and TG curves. As depicted in Figures 12a and 10b, it is evident that the incorporation of photosensitizer 819 does not influence the thermal curing behavior of ALSZ. No significant changes are observed in terms of the thermal curing weight loss (−36.34%) and curing temperature (225 °C).

Subsequently, ALSZ(10:1)−1%819−0.25%cumenyl−1% CoCPA (synergistic photothermocuring; exposure to 405 nm light for 1 min before heating) and ALSZ(10:1)−0.25% cumenyl−1%CoCPA (catalytic thermocuring, directly heating without light exposure) were cured into solid, and the ceramic conversion yield at 800 °C was measured by TGA. The resulting curve is presented in Figure 12c. Clearly, the addition of photosensitizer 819 moderately enhances the ceramic conversion yield from 71.03 to 76.39%. These results open a window for ALSZ to be utilized in the fields of additive manufacturing for ceramic metastructure and fiber prepregs for laminate-type composites.

Digital light processing (DLP) is one of the additive manufacturing methods of thermosetting preceramics and their slurry for ceramic metamaterials through pyrolysis. Other than the conventional blending of photosensitive polymers with polysilazanes, ALSZ, as a single-component and reactive acryl-grafted liquid preceramic, is an ideal candidate for DLP printing to fabricate preceramic-based metamaterials and final ceramic metamaterials.

In the traditional prepreg processing for laminate composites, the precise regulation of temperature and time during thermal curing should be carried out cautiously to ensure optimal resin−fiber contact and minimize pore formation.[28] By employing the photocuring prepreg process,[29] a prepreg with high quality can be cost-efficiently fabricated through the convenient adjustment of light power and the exposure duration at ambient temperature.[19,20] In this paper, the single-component photocurable ALSZ offers a competitive solution for prepreg processing in the manufacture of laminate composites.

3.5. Catalytic Thermocuring Mechanism of ALSZ. The comprehension of probable mechanisms in the catalytic thermocuring of ALSZ is important for the further molecular design and determination of the curing schedule of the studied preceramics. The FT-IR spectra of the ALSZ(10:1)−1% cumenyl−0.5%CoCPA system heat-treated under an Ar atmosphere at different temperatures are shown in Figure 13a. The characteristic absorption bands assigned to N−H (3382 cm^{-1}), H−CH_2 (2960 cm^{-1}), Si−H (2124 cm^{-1}), C═C (1600 cm^{-1}), and Si−C(1260 cm^{-1})[13] were recognized. With an increase in the heat treatment temperature, the absorption peaks of N−H, Si−H, and C═C decreased gradually at discriminative degrees. Using the Si−C peak at 1260 cm^{-1} as the internal standard, the relative absorbance ratio (e.g., for Si−H at 2124 cm^{-1}, the relative absorbance ratio is A_{2124}/A_{1260}) versus the heat treatment temperature is plotted in Figure 13b. According to the figure, the reaction of N−H and C═C occurs at lower temperatures, and the curing

https://doi.org/10.1021/acsomega.4c02018
ACS Omega 2024, 9, 24959−24969

reaction of Si−H can proceed in a wide temperature range from low to high temperatures. These findings agree well with the results obtained from the DSC results discussed above.

The reactions that occur during the catalytic thermocuring are shown in Figure 14. First, the radical initiators decompose to form radicals, and conventional radical polymerization occurs.[30,31] Second, cobalt(II) naphthenate acid can reduce cumene hydroperoxide to generate free radicals at low temperatures, so redox radical polymerization can proceed at comparably low temperatures.[32,33] At the same time, transamination condensations occur between the -Si−NH- units to form branched crosslinking silazane networks, together with the release of ammonia gas.[34] With further increase in the temperature, dehydrogenation polycondensation will occur between Si−H and N−H (or between Si−H bonds) in the system under catalysis of many transition metal compounds;[35,36] to the best of our knowledge, the high activity of nickel naphthenate or cobalt naphthenate for PSZ dehydrocoupling in this paper is first found and investigated. In summary, the mechanism of catalytic thermocuring involves multiple reactions and is comparably complex, and the final solidification of ALSZ is realized by their synergistic polymerization.

4. CONCLUSIONS

Single-component acrylate-grafted oligosilazane resins were successfully synthesized by hydrogen-transfer addition between LSZ and 2-isocyanatoethyl acrylate at ambient conditions. Under the assistance of cumene hydroperoxide and a metal catalyst (NiCPA or CoCPA), the curing temperature of ALSZs is decreased drastically, and weight loss in curing is reduced sharply, implying the efficient catalytic thermocuring of ALSZ. Synergistic photothermocuring of ALSZ is readily completed by combining a radical initiator, a transition metal catalyst, and a photosensitizer, showing the advantages of material shaping at RT and minimal weight loss during subsequent thermal curing. The curing mechanism revealed by the FT-IR study is deemed to involve multiple reactions of acrylate, silicon−H, and silicon−NH-. The cured ALSZs exhibit a high ceramic yield (71−75.7% at 800 °C). The pyrolysis ceramic retained its original shape. The single-component acrylate-grafted oligosilazane synthesized in this study exhibits promising application potential as an ideal candidate for thermosetting ceramic precursors and meets the demands of material processes of light additive manufacturing and prepreg laminates.

AUTHOR INFORMATION

Corresponding Author

Mingcun Wang − *School of Chemistry, Beihang University, Beijing 102206, China;* orcid.org/0000-0002-6254-1633; Email: mcwang@buaa.edu.cn

Authors

Keke Pei − *School of Chemistry, Beihang University, Beijing 102206, China*

Sen Li − *School of Chemistry, Beihang University, Beijing 102206, China*

Biwen Cao − *Xi'an Aerospace Composites Research Institute, Xi'an, Shaanxi Province 710025, China*

Mingjie Liu − *School of Chemistry, Beihang University, Beijing 102206, China;* orcid.org/0000-0002-8399-2134

Complete contact information is available at: https://pubs.acs.org/10.1021/acsomega.4c02018

Notes

The authors declare no competing financial interest.

ACKNOWLEDGMENTS

The statements made herein are solely the responsibility of the authors. This research was made possible by financial support from the Xi'an Aerospace Composites Research Institute of CASC with contract number H2021120003.

ABBREVIATIONS

ALSZ, acrylate-grafted liquid oligosilazane; TGA, thermogravimetric analysis; DSC, differential scanning calorimetry; TMA, thermomechanical analysis; PIP, precursor infiltration and pyrolysis; CoCPA, cobalt naphthenate acid; NiCPA, nickel naphthenate acid; Cumenyl, cumene hydroperoxide

REFERENCES

(1) Fang, G.; Gao, X.; Song, Y. A Review on Ceramic Matrix Composites and Environmental Barrier Coatings for Aero-Engine: Material Development and Failure Analysis. *Coatings* **2023**, *13* (2), 357−374.

(2) Jia, D.; Liang, B.; Yang, Z.; Zhou, Y. Metastable Si-B-C-N ceramics and their matrix composites developed by inorganic route based on mechanical alloying: Fabrication, microstructures, properties and their relevant basic scientific issues. *Prog. Mater. Sci.* **2018**, *98*, 1−67.

(3) Huang, J.; Liu, R.; Hu, Q.; et al. High temperature abradable sealing coating for SiCf/SiC ceramic matrix composites. *Ceram. Int.* **2023**, *49* (2), 1779−1790.

(4) Hu, Q.; Zhou, X.; Tu, Y.; et al. High-temperature mechanical properties and oxidation resistance of SiCf/SiC ceramic matrix composites with multi-layer environmental barrier coatings for turbine applications. *Ceram. Int.* **2021**, *47* (21), 30012−30019.

(5) Shi, W.; Zhang, C.; Wang, B.; et al. Mode I interlaminar fracture toughness of two-dimensional continuous fiber reinforced ceramic matrix composites using wedge-loaded double cantilever beam method. *Composites, Part A* **2023**, *168*, 107466−107475.

(6) Lyu, Y.; Cheng, Y.; Zhao, G.; et al. Modification of SiBCN by Zr atom and its effect on ablative resistance of Cf/SiBCN (Zr) composites. *Composit. B-Eng.* **2023**, *253*, 110511−110522.

(7) Yu, Z.; Yang, L.; Zhan, J.; et al. Preparation, cross-linking and ceramization of AHPCS/Cp2ZrCl2 hybrid precursors for SiC/ZrC/C composites. *J. Eur. Ceram. Soc.* **2012**, *32* (6), 1291−1298.

(8) Liang, B.; Yang, Z.; Li, Y.; et al. Ablation behavior and mechanism of SiCf/Cf/SiBCN ceramic composites with improved thermal shock resistance under oxyacetylene combustion flow. *Ceram. Int.* **2015**, *41* (7), 8868−8877.

(9) Mainzer, B.; Chaorong, Lin.; Raouf, J.; et al. Characterization and application of a novel low viscosity polysilazane for the manufacture of C- and SiC-fiber reinforced SiCN ceramic matrix composites by PIP process. *J. Eur. Ceram. Soc.* **2019**, *39* (2−3), 212−221.

(10) Santhosh, U.; Unni, S.; Ahmad, J.; Jlees, A.; Easler, T.; Timothy, E. A polymer infiltration and pyrolysis (PIP) process model for ceramic matrix composites (CMCs). *J. Am. Ceram. Soc.* **2021**, *104* (12), 6108−6130.

(11) Luo, X.; Li, X.; Bao, Z.; et al. Preparation of SiCN ceramic fibres via UV irradiation curing polysilazane. *Bulletin Mater. Sci.* **2023**, *46* (2), 111−117.

(12) Wang, M.; Ning, Y.; Han, W.; Zhao, T. Oligosilazane cured by moisture as fluorine-free hydrophobic coating for waterproof polymer-matrix composite materials. *J. Coat. Technol. Res.* **2018**, *15* (6), 1251−1258.

(13) Yang, J.; Wen, Q.; Feng, B.; et al. Microstructural evolution and electromagnetic wave absorbing performance of single-source-precursor-synthesized SiCuCN-based ceramic nanocomposites. *J. Adv. Ceram.* **2023**, *12* (7), 1299−1316.

https://doi.org/10.1021/acsomega.4c02018
ACS Omega 2024, 9, 24959−24969

(14) Zhang, Q.; Jia, D.; Yang, Z.; et al. Synthesis of Novel Cobalt-Containing Polysilazane Nanofibers with Fluorescence by Electrospinning. *Polymers* **2016**, *8* (10), 350−362.
(15) Xuan, L.; Li, D.; Wang, M. Propargyloligosilazane matrixed composite for high temperature material combining polymer and ceramic properties. *Int. J. Chem. Reactor Eng.* **2021**, *19* (3), 277−285.
(16) Huang, X.; Wang, D.; Hu, L.; et al. Pyrolyzing preceramic polymer into ceramic reverses the wettability of the extreme wetting surface and enhances mechanical abrasion resistance. *Ceram. Int.* **2019**, *45* (2), 2053−2059.
(17) Zhan, Y.; Li, W.; G, R.; et al. Rapid curing of polysilazane coatings at room temperature via chloride-catalyzed hydrolysis/condensation reactions. *Prog. Org. Coat.* **2022**, *167*, 106872−106878.
(18) Li, S.; Duan, W.; Zhao, T.; et al. The fabrication of SiBCN ceramic components from preceramic polymers by digital light processing (DLP) 3D printing technology. *J. Eur. Ceram. Soc.* **2018**, *38* (14), 4597−4603.
(19) Chen, S.; Wan, X.; Li, J.; et al. Fabrication of electrical semiconductive SiCN ceramics by vat photopolymerization. *J. Mater. Sci. Technol.* **2023**, *165*, 123−131.
(20) Hoffmann, M.; Zahedtalaban, M.; Denk, J.; et al. Photoinduced thiol-ene click chemistry for resource-efficient curing of polysilazane-based coatings and its effects on coating property profile. *Open Ceram.* **2023**, *15*, 100384−100393.
(21) Ren, D.; Xu, W.; Gao, Y.; Wang, Y. UV curing behavior of a liquid polyborosilazane and stereolithography to SiBCN ceramic components. *Ceram. Int.* **2023**, *49* (7), 11571−11578.
(22) Graeme, M.; David, H. S. *The Chemistry of Radical Polymerization*; Elsevier Science Ltd, 2005.
(23) Arar, A.; Ahmad, A.; Mousawi, A. A.; Assi, A. M.; Morlet-Savary, F.; Fabrice, M. Peroxide-free redox initiating systems for polymerization in mild conditions. *Polym. Chem.* **2021**, *12* (12), 1816−1822.
(24) Laine, R. M. Transition metal catalysed synthesis of oligo- and polysilazanes. *Platinum Met. Rev.* **1988**, *32* (2), 64−71.
(25) Huang, C.; Wang, Z.; Wang, M. Catalysis of nickel acetylacetonate in thermal cure and ceramization of SiC preceramic resin. *J. Organomet. Chem.* **2016**, *804*, 123−131.
(26) Ai, T.; Zhang, Y.; Zhong, D.; et al. Hybrids from silazane and allyl-containing benzoxazine for low-curing temperature and high-flame retardance. *J. Appl. Polym. Sci.* **2022**, *139* (11), 51801−51809.
(27) Zanchetta, E.; Marco, C.; Giorgia, F.; et al. Stereolithography of SiOC ceramic microcomponents. *Adv. Mater.* **2016**, *28* (2), 370−376.
(28) Netzel, C.; Hoffmann, D.; Battley, M.; et al. Effects of environmental conditions on uncured prepreg characteristics and their effects on defect generation during autoclave processing. *Compos. - A: Appl. Sci. Manuf.* **2021**, *151*, 106636−106649.
(29) Quan, D.; Deegan, B.; Binsfeld, L.; et al. Effect of interlaying UV-irradiated PEEK fibres on the mechanical, impact and fracture response of aerospace-grade carbon fibre/epoxy composites. *Composites, Part B* **2020**, *191*, 107923−107935.
(30) D'Elia, R.; Gilles, D.; Sylvie, D.; et al. Cure kinetics of a polysilazane system: Experimental characterization and numerical modelling. *Eur. Polym. J.* **2016**, *76*, 40−52.
(31) Morales, A.; Pojman, J. A. A study of the effects of thiols on the frontal polymerization and pot life of multifunctional acrylate systems with cumene hydroperoxide. *J. Polym. Sci. A Polym. Chem.* **2013**, *51* (18), 3850−3855.
(32) Turovskij, N.; Nikolaj, T.; Raksha, E.; Elena; Berestneva, Y.; Yuliya, B. Anion effect on the cumene hydroperoxide decomposition in the presence of Cu (II) 1,10-phenanthrolinates. *J. Organomet. Chem.* **2020**, *922*, 121371−121374.
(33) Xu, X.; He, J.; Zeng, Y.; et al. Controllable surface-initiated metal-free atom transfer radical polymerization of methyl methacrylate on mesoporous SBA-15 via reductive quenching. *Eur. Polym. J.* **2020**, *131*, 109724−109730.
(34) Günthner, M.; Wang, K.; Wang, K.; Bordia, R. K.; Motz, G. Conversion behaviour and resulting mechanical properties of polysilazane-based coatings. *J. Eur. Ceram. Soc.* **2012**, *32* (9), 1883−1892.
(35) Chow, A. W.; Hamlin, R. D.; Blum, Y.; Laine, R. M. Polymerization kinetics of polysilazane by transition metal catalyzed dehydrocoupling reaction. *J. Polym. Sci. Polym. Lett. Ed.* **1988**, *26* (2), 103−108.
(36) Blum, Y.; Laine, R. M. Catalytic methods for the synthesis of oligosilazanes. *Organometallics* **1986**, *5* (10), 2081−2086.

https://doi.org/10.1021/acsomega.4c02018
ACS Omega 2024, 9, 24959−24969